# A Mechanism for Ion Selectivity in Potassium Channels: Computational Studies of Cation-π Interactions

Robert A. Kumpf and Dennis A. Dougherty*

A combination of computational methods has been used to evaluate the interaction between the π face of a benzene molecule and the monovalent cations of lithium, sodium, potassium, and rubidium. In the gas phase, the ions are strongly bound, and the affinity for benzene follows the expected electrostatic trend (lithium, largest; rubidium, smallest). However, in an aqueous environment, a reordering occurs such that the potassium ion is preferred over all the other ions for 2:1 benzene:ion complexes. The selectivity sequence parallels that seen in voltage-gated potassium channels. Given that several conserved aromatic residues are present in the pore region of such channels, these results suggest that the cation-π interaction may be responsible for the ion selectivity in potassium channels.

The current interest in $K^+$ channels, which has followed the successful molecular cloning of the *shaker* gene of *Drosophila*, has produced many valuable and often surprising insights (*1*, *2*). The channel is a homotetramer, with each subunit containing six putative membrane-spanning helices and a "pore" region, which lies between the fifth and sixth transmembrane helices and delineates the ion channel (*3*). An important feature of the *shaker* channel and related structures is their considerable ion selectivity; $K^+$ is preferred over $Na^+$ and $Li^+$ by a large margin and over larger ions such as $Rb^+$ to a smaller but still significant extent (*2*). A major challenge in the ion channel field is the identification of the molecular interactions responsible for this selectivity. In this context, we, and no doubt others, were intrigued by the amino acid sequences of these channels in the pore region. In *shaker*, the sequence is . . . **AFW**WAVV**T**M**TT**V**GYGD**MT. . . (boldface indicates generally conserved residues) (*4*). From our perspective, the sequence is surprisingly hydrophobic in comparison to what might have been expected for a cation channel. Of special interest to us were the large number of conserved aromatic residues (F, Y, and W) in the pore.

The aromatic residues caught our attention because of our long-standing interest in the "cation-π" interaction (*5*, *6*) (Scheme 1). This is the stabilizing interaction between a cation and the electron-rich face of an aromatic ring.

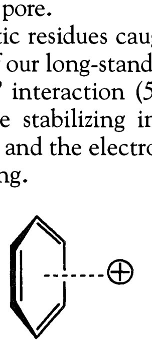

**Scheme 1.** The cation-π interaction.

Such interactions have been observed in the gas phase (*7*, *8*) and in the "amino-aromatic" interaction noted in protein crystal structures by Burley and Petsko (*9*). We have shown, using a series of synthetic receptors, that this effect can provide a quite powerful force for molecular recognition in aqueous media (*6*). On the basis of these model studies, we proposed (*5*) that the cation-π interaction would be important in binding the positive charge of the neurotransmitter acetylcholine (ACh). This suggestion has received considerable support from studies of ACh receptors (*10*) and the crystal structure of the ACh esterase (*11*). In addition, cation-π interactions are thought to be important in the binding of more hydrophilic cations, such as the guanidinium ion of Arg (*12*), and $RNH_3^+$ groups of neurotransmitters, such as norepinephrine, dopamine, and serotonin (*13*).

Here, we explore the possible role of the cation-π interaction with regard to the ion selectivity of the *shaker* channel. In particular, we evaluate the cation-π interaction of the monovalent ions $Li^+$, $Na^+$, $K^+$, and $Rb^+$ in aqueous media. Our studies are computational in nature and involve simple models compared with the actual channel. Despite the simplicity of these models, we believe the results provide strong permissive evidence for the involvement of the cation-π interaction in establishing the ion selectivity of $K^+$ channels.

We performed two series of simulations, one on $M^+\cdots$benzene complexes and one on benzene$\cdots M^+ \cdots$benzene complexes, where $M^+ = Li^+, Na^+, K^+$, and $Rb^+$ (Fig. 1). Benzene is the prototypical aromatic group and thus serves as a model for the π systems of the amino acid sidechains of Phe, Tyr, and Trp. An absolute $M^+\cdots$benzene binding energy in the gas phase was obtained by ab initio quantum mechanical methods (*14*) with optimization of the distance between $M^+$ and the centroid of the benzene ring. This produces binding energies, $\Delta E^{\text{bind}}$, for the various ions. Similar calculations were performed for the benzene$\cdots M^+ \cdots$benzene complexes (Table 1).

To evaluate aqueous solvation effects, we conducted Monte Carlo simulations using statistical perturbation theory to evaluate the relative solvation free energies of pairs of species, expressed as $\Delta G^{\text{sol}}$ (*15*). Simulations were carried out on both the naked ions and the ion-benzene complexes. Combination of the calculated results, according to the equation given in Fig. 1, provides $\Delta\Delta G_{\text{aq}}$, the relative stability of a pair of $M^+\cdots$benzene complexes in water. For the benzene$\cdots M^+ \cdots$benzene complexes, two versions of the same scheme were used. In model I, each complex was considered at its optimal gas-phase benzene$\cdots$benzene separation. In model II, the benzene$\cdots$benzene separation was fixed at the optimal $K^+$ distance for comparison with $Li^+$ and $Na^+$; for the $K^+$-$Rb^+$ comparison, the $Rb^+$ distance was used. These models mimic two limiting cases: One where the channel is completely free to adjust to the different sizes of the various ions, and one where it is locked into a geometry that is optimal for the larger ion of the pair. The results of the calculations are summarized in Fig. 2.

Several aspects of the data deserve further comment. First, in the gas phase, the $M^+\cdots$benzene binding sequence (Table 1) is $Li^+ > Na^+ > K^+ > Rb^+$ for both 1:1 and 2:1 complexes. This is the sequence seen in conventional electrostatic binding. In fact, a linear relation can be obtained between $M^+\cdots$benzene and $M^+\cdots Cl^-$ binding energies.

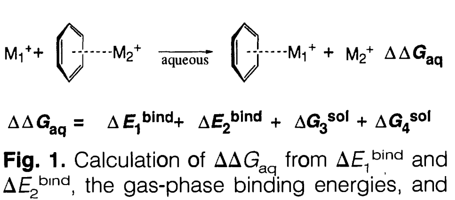

$$\Delta\Delta G_{\text{aq}} = \Delta E_1^{\text{bind}} + \Delta E_2^{\text{bind}} + \Delta G_3^{\text{sol}} + \Delta G_4^{\text{sol}}$$

**Fig. 1.** Calculation of $\Delta\Delta G_{\text{aq}}$ from $\Delta E_1^{\text{bind}}$ and $\Delta E_2^{\text{bind}}$, the gas-phase binding energies, and $\Delta G_3^{\text{sol}}$ and $\Delta G_4^{\text{sol}}$, the relative aqueous solvation free energies. We have assumed that entropic and vibrational contributions to the binding energies are similar for all of the complexes, which is supported by experimental data (*7*).

---

Arnold and Mabel Beckman Laboratories of Chemical Synthesis, Division of Chemistry and Chemical Engineering, California Institute of Technology, Pasadena, CA 91125.

*To whom correspondence should be addressed.

**Fig. 2.** Values of $\Delta\Delta G_{aq}$ (in kilocalories per mole with one standard deviation). A positive number indicates $K^+$ binding is preferred. The actual reactions studied correspond to the bottom reaction in Fig. 1: The spectator ions are omitted here. For the 2:1 complexes, the top value corresponds to model I, and the number in parentheses refers to model II.

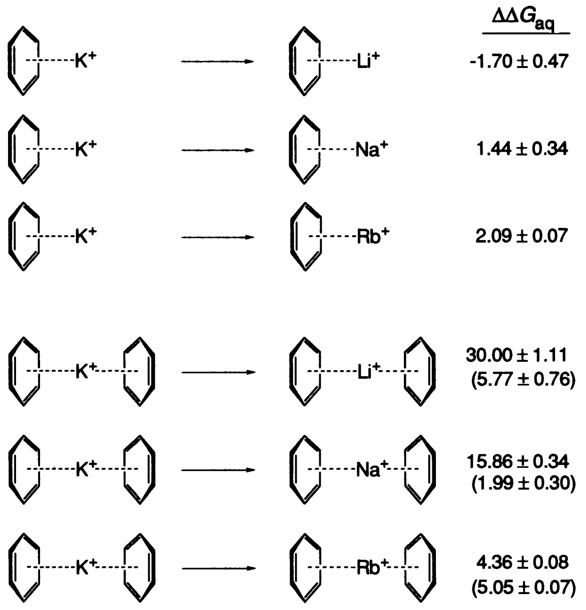

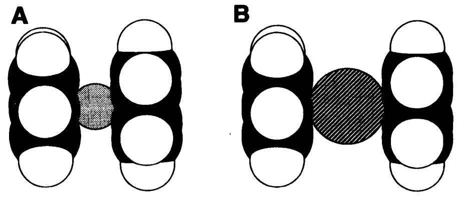

**Fig. 3.** Optimized benzene···$M^+$···benzene complexes for model I where (**A**) M = Li and (**B**) M = K.

Thus, in the gas-phase cation-π interaction, benzene behaves much like a weak anion.

A change to an aqueous environment causes a surprising reordering to occur. For the $M^+$···benzene complexes, $K^+$ is preferred over $Na^+$ and $Rb^+$. The smallest ion, $Li^+$, is still the best ligand for benzene. However, even this preference is reversed for the benzene···$M^+$···benzene complexes, and $K^+$ is preferred over all the other ions (Fig. 2).

This result can be rationalized with reference to the extreme comparison of $Li^+$ versus $K^+$. In the benzene···$Li^+$···benzene complex (Fig. 3A), the benzene···benzene distance in model I is small enough that no water molecules (which are about the size of $K^+$) can solvate the $Li^+$. Thus, two benzene rings completely remove the first aqueous solvation shell of $Li^+$, and the energetic penalty for desolvation is large. In the benzene···$K^+$···benzene complex (Fig. 3B), there is space for some direct aqueous solvation of the $K^+$. Thus, although the interaction with the benzene is weaker than in the $Li^+$ case, the desolvation penalty is less, and $K^+$ is preferred. In model II, where the benzene···benzene distance is fixed at that for the $K^+$ complex (perhaps a situation more relevant to a $K^+$ channel), solvation of the $Li^+$ is improved, but the $K^+$ complex is still preferred. Note that in this case, the $Li^+$ is very much off center (Table 1), strongly bound to one benzene but weakly bound to the other. This type of reasoning is fully supported by the radial distribution functions from the Monte Carlo simulations. The data for the other ions can be rationalized with a similar balance of binding and desolvation effects.

The calculations we describe represent the state-of-the-art in liquid simulations, and we are confident that the fundamental conclusion concerning a reversal of ion selectivities in water versus the gas phase is correct. Theories of ion permeability, such as Eisenman theory (*16*), invariably invoke a balance of two forces: that of a binding interaction between the ion and some site(s) in the channel, and that of the desolvation of the ion. It has been known for some time that almost any ion selectivity sequence can be obtained if a proper balance is struck. What we provide here is a molecular description of a specific interaction that appears to lead naturally to the kinds of selectivity seen in $K^+$ channels (*17*, *18*).

The issue of biological relevance is complex. Our calculations emphasize the roles of binding and desolvation, and there is evidence that these are important in the actual channel as well. Streaming potential measurements (*19*) suggest that $K^+$ is substantially desolvated as it traverses the membrane. Consequently, direct interactions with some site(s) in the pore region would seem to be essential. Because the actual channel is a tetramer, we feel that an attractive model for the selectivity filter would involve a ring of aromatic residues located at a constricted region of the pore. Thus, the $K^+$ could be coordinated by four aromatic rings in an equatorial plane, with water molecules occupying the two axial positions. In fact, recent computational models for the full $K^+$ channel (*20*, *21*) do indicate a prominent role for aromatic residues in the establishment of the selectivity filter. One model (*20*) explicitly proposes a ring of tyrosines (from the GYG sequence), and the authors suggest that cation-π interactions might be involved. We provide a physical basis for such an arrangement producing $K^+$ selectivity. Of course, our calculations provide only permissive evidence for the operation of cation-π interactions in the determination of the ion selectivity of voltage-gated potassium channels, and we look forward to further experimental studies of intact channels to confirm or deny its role.

**Table 1.** Gas-phase binding data. All binding energies, which are reported as absolute values, are negative (thermodynamically favorable).

| Ion | Ionic radius* (Å) | Aqueous solvation energy (kcal/mol) | $M^+$···$Cl^-$ binding energy† (kcal/mol) | 1:1 complexes | | 2:1 complexes | | | |
|---|---|---|---|---|---|---|---|---|---|
| | | | | | | Model I | | Model II | |
| | | | | $\Delta E^{bind}$ (kcal/mol) | r (Å)‖ | $\Delta E^{bind}$ (kcal/mol) | r (Å)‖ | $\Delta E^{bind}$ (kcal/mol) | r (Å)‖ |
| $Li^+$ | 0.60 | 122 | 153 | 39.5‡ | 1.96 | 65.1 | 2.12 | 47.7 | 2.09, 3.75 |
| $Na^+$ | 0.95 | 98 | 134 | 24.4 | 2.41 | 44.9 | 2.48 | 38.6 | 2.85, 2.99 |
| $K^+$ | 1.33 | 81 | 120 | 19.2§ | 2.88 | 35.9 | 2.92 | 35.4 | 3.03 |
| $Rb^+$ | 1.48 | 75 | 115 | 15.8 | 2.96 | 28.7 | 3.03 | 28.7 | 3.03 |

*From (*2*). †Equal to the gas-phase, heterolytic bond dissociation energy of MCl. ‡Experimental change in enthalpy $-\Delta H$ = 38.3 kcal/mol [calculated with data from (*8*), assumes a change in entropy $\Delta S^0$ = 23 entropy units]. §Experimental $-\Delta H$ = 19.2 kcal/mol (corrected value = 18.3 kcal/mol) (*7*). ‖Distance from $M^+$ to center of benzene ring. Two values indicate asymmetric placement of ion.

## REFERENCES AND NOTES

1. C. Miller, *Science* **252**, 1092 (1991).
2. B. Hille, *Ionic Channels of Excitable Membranes* (Sinauer, Sunderland, MA, 1992).
3. G. Yellen, M. E. Jurman, T. Abramson, R. MacKinnon, *Science* **251**, 939 (1991); R. MacKinnon and G. Yellen, *ibid.* **250**, 276 (1990); A. J. Yool and T. L. Schwarz, *Nature* **349**, 700 (1991); R. MacKinnon, *ibid.* **350**, 232 (1991).
4. For a large number of pore sequences, see M. P. Kavanaugh *et al.*, *J. Biol. Chem.* **266**, 7583 (1991). The very recently sequenced inward-rectifier K$^+$ channels are quite different in structure from A-type K$^+$ channels, but are highly conserved in the pore. The GYG sequence is conserved, and FLF replaces FWW. See K. Ho *et al.*, *Nature* **362**, 31 (1993); Y. Kubo, T. J. Baldwin, Y. N. Jan, L. Y. Jan, *ibid.*, p. 127. Similarly, in the very recently sequenced calcium-dependent K$^+$ channel mSlo, the GYG is conserved, but VYL appears to align with the FWW. See A. Butler, S. Tsunoda, D. P. McCobb, A. Wei, L. Salkoff, *Science* **261**, 221 (1993). Abbreviations for the amino acid residues are A, Ala; D, Asp; F, Phe; G, Gly; L, Leu; M, Met; T, Thr; V, Val; W, Trp; and Y, Tyr.
5. D. A. Dougherty and D. A. Stauffer, *Science* **250**, 1558 (1990).
6. M. A. Petti, T. J. Shepodd, R. E. Barrans Jr., D. A. Dougherty, *J. Am. Chem. Soc.* **110**, 682 (1988).
7. J. Sunner, K. Nishizawa, P. Kebarle, *J. Phys. Chem.* **85**, 1814 (1981).
8. R. W. Taft *et al.*, *Pure Appl. Chem.* **62**, 17 (1990).
9. S. K. Burley and G. A. Petsko, *FEBS Lett.* **203**, 139 (1986). See also M. Perutz *et al.*, *J. Am. Chem. Soc.* **108**, 1064 (1986); M. Levitt and M. Perutz, *J. Mol. Biol.* **201**, 751 (1988).
10. J.-P. Changeux, A. Devillers-Thiéry, J.-L. Galzi, D. Bertrand, *TiPS* **13**, 299 (1992).
11. J. L. Sussman *et al.*, *Science* **253**, 872 (1991).
12. V. Chaturvedi, D. L. Donnelly-Roberts, T. L. Lentz, *Biochemistry* **31**, 1370 (1992); M. H. le Du, P. Marchot, P. E. Bougis, J. C. Fontecilla-Camps, *J. Biol. Chem.* **267**, 22122 (1992); T. L. Lentz, *Biochemistry* **30**, 10949 (1991).
13. S. Trumpp-Kallmeyer, J. Hoflack, A. Bruinvels, M. Hibert, *J. Med. Chem.* **35**, 3448 (1992).
14. Ab initio molecular orbital calculations (*22*) were performed with either the Gaussian 90 (*23*) or Gaussian 92 program (*24*). Calculations for benzene were carried out at the 6-31G**//6-31G** level, whereas a mixed basis set (6-31G** for C and H; STO-3G* for M$^+$) was used for all of the 1:1 and 2:1 complexes. Calculations were in good agreement with full 6-31G**//6-31G** results for the 1:1 complexes of benzene with Li$^+$ and Na$^+$ and with experimental data for the Li$^+$ and K$^+$ complexes (Table 1). For the 1:1 complexes, benzene was fixed at its 6-31G**//6-31G** geometry, and the M$^+\cdots$benzene intermolecular separation was optimized in $C_{6v}$ symmetry. For both models used in the calculations of the 2:1 complexes, the cation was sandwiched between two staggered, face-to-face benzene molecules (each fixed at the 6-31G**//6-31G** monomer geometry) along the vector connecting the centroids of the rings. Model I maintained $D_{6d}$ symmetry constraints, whereas in model II, $C_{6v}$ symmetry was maintained. These calculated gas-phase structures were then used in the solution studies.
15. All solution studies were performed at constant temperature (298 K) and pressure (1 atm) with the use of statistical perturbation theory (*25*) and the program BOSS (*26*). The complexes were treated as a single solute and placed at the center of a box 20 Å on a side containing 260 TIP3P water (*27*) molecules. Periodic boundary conditions were applied, and an 8.5 Å cutoff was used. A series of four simulations with double-wide sampling were performed for each system with $9 \times 10^5$ steps of equilibration, followed by averaging over $2 \times 10^6$ configurations. The OPLS parameters for benzene were optimized previously for benzene-water simulations (*28*), and parameters for the cations M$^+$ had been optimized to reproduce relative hydration energies (*29*). The high quality of these parameters is seen in a comparison of the calculated and experimental relative aqueous solvation energies (respectively, in kilocalories per mole): Li$^+$/Na$^+$, 24.5 versus 23.9; Na$^+$/K$^+$, 17.0 versus 17.6; and K$^+$/Rb$^+$, 5.6 versus 5.1. However, when used to calculate gas-phase M$^+\cdots$benzene binding energies, the OPLS parameters give poor quantitative agreement with the ab initio results. As such, we felt it would be inappropriate to relax the M$^+\cdots$benzene distance during the aqueous simulations because the OPLS parameters may lead to incorrect energies or geometries. Thus, we adopted a combined approach (Fig. 1) in which the binding energies were taken from the gas-phase calculations, and statistical perturbation theory was used to determine the relative solvation energies of the various species with fixed geometries. Relative free energies of hydration were determined through stepwise perturbation of one alkali metal complex into another. Because the overall perturbations were relatively small, a fairly large step size ($\lambda = 0.125$) was used. Perturbations in the 1:1 complexes involved the mutation of Na$^+$ to Li$^+$ and K$^+$ to Na$^+$ and Rb$^+$. In a similar fashion, K$^+$ was changed to Li$^+$, Na$^+$, and Rb$^+$ in the 2:1 complexes.
16. G. Eisenman, in *Symposium on Membrane Transport and Metabolism*, A. Kleinzeller and A. Kotyk, Eds. (Academic Press, New York, 1961), p. 163; ______ and R. Horn, *J. Membr. Biol.* **76**, 197 (1983).
17. For an alternative model emphasizing carbonyl groups as the selectivity filter, see J. Wu, *Biophys. J.* **60**, 238 (1991). For other discussions of the possible role of carbonyl oxygens in the provision of ion binding sites, see G. Eisenman and S. J. Krasne, in *MTP International Review of Science, Biochemistry Series*, C. F. Fox, Ed. (Butterworths, London, 1975), vol. 2, p. 27; G. Eisenman, O. Alvarez, J. Aqvist, *J. Inclusion Phenom. Mol. Recognition Chem.* **12**, 23 (1992).
18. Recently, it has been proposed that a cation binding site can be formed from phenylalanine side chains in the ion channel of the nicotinic ACh receptor. G. Eisenman, A. Villarroel, M. Montal, O. Alvarez, in *Progress in Cell Research*, J. M. Ritchie, P. J. Magistretti, L. Bolis, Eds. (Elsevier, New York, 1990), vol. 1, p. 195.
19. C. Miller, *Biophys. J.* **38**, 227 (1982).
20. S. R. Durell and H. R. Guy, *ibid.* **62**, 238 (1992).
21. S. Bogusz, A. Boxer, D. D. Busath, *Protein Eng.* **5**, 285 (1992).
22. W. J. Hehre, L. Radom, P. v. R. Schleyer, J. A. Pople, *Ab Initio Molecular Orbital Theory* (Wiley, New York, 1986).
23. Gaussian 90: M. J. Frisch *et al.*, Gaussian, Inc., Pittsburgh, PA, 1990.
24. Gaussian 92, revision A: M. J. Frisch *et al.*, Gaussian, Inc., Pittsburgh, PA, 1992.
25. R. W. Zwanzig, *J. Chem. Phys.* **22**, 1420 (1954); D. L. Beveridge and F. M. DiCapua, *Annu. Rev. Biophys. Biophys. Chem.* **18**, 431 (1989); W. L. Jorgensen, *J. Am. Chem. Soc.* **111**, 3770 (1989); *Acc. Chem. Res.* **22**, 184 (1989).
26. BOSS, version 2.7; W. L. Jorgensen, Yale University, New Haven, CT, 1989.
27. W. L. Jorgensen, J. Chandrasekhar, J. D. Madura, R. W. Impey, M. L. Klein, *J. Chem. Phys.* **79**, 926 (1983).
28. W. L. Jorgensen and D. L. Severance, *J. Am. Chem. Soc.* **112**, 4768 (1990).
29. J. Åqvist, *J. Phys. Chem.* **94**, 8021 (1990).
30. We thank W. Jorgensen for providing the BOSS program and for advice on parameters and H. Lester and R. MacKinnon for helpful discussions. Supported by the Office of Naval Research. Contribution no. 8759 from the Division of Chemistry and Chemical Engineering, California Institute of Technology.

20 April 1993; accepted 28 July 1993

---

# Unusual Radar Echoes from the Greenland Ice Sheet

E. J. Rignot, S. J. Ostro, J. J. van Zyl, K. C. Jezek

**Airborne radar images of part of the Greenland ice sheet reveal icy terrain whose radar properties are unique among radar-studied terrestrial surfaces but resemble those of Jupiter's icy Galilean satellites. The 5.6- and 24-centimeter-wavelength echoes from the Greenland percolation zone, like the 3.5- and 13-centimeter-wavelength echoes from the icy satellites, are extremely intense and have anomalous circular and linear polarization ratios. However, the detailed subsurface configurations of the Galilean satellite regoliths, where heterogeneities are the product of prolonged meteoroid bombardment, are unlikely to resemble that within the Greenland percolation zone, where heterogeneities are the product of seasonal melting and refreezing.**

It has been known since the 1970s that radar echoes from the icy Galilean satellites are extraordinary (*1*). The radar reflectivities (*2*) of Europa, Ganymede, and Callisto are several orders of magnitude greater than those recorded for comets, the moon, the inner planets, and nonmetallic asteroids, and they show little dependence on the radar wavelength. In addition, the circular polarization ratios $\mu_C$ of the icy satellites (*3*) exceed unity ($\mu_C$ is less than 0.4 for most other planetary targets), and their linear polarization ratios $\mu_L$ are ~0.5 (also larger than values for other planets) (*4*). More recently, radar observations of the residual south polar ice cap of Mars (*5*), portions of Titan (*6*), and polar caps on Mercury (*7*) have revealed that surfaces with high radar reflectivity and $\mu_C > 1$ exist elsewhere in the solar system.

Here we report the measurement of similarly exotic radar signatures for icy surfaces on Earth. The observations were collected in June 1991 by the National Aeronautics and Space Administration (NASA)–Jet

---

E. J. Rignot, S. J. Ostro, J. J. van Zyl, Jet Propulsion Laboratory, California Institute of Technology, Pasadena, CA 91109.
K. C. Jezek, Byrd Polar Research Center, Ohio State University, Columbus, OH 43210.